PHYSICAL REVIEW B VOLUME 28, NUMBER 5 1 SEPTEMBER 1983

Rapid Communications

The Rapid Communications section is intended for the accelerated publication of important new results. Manuscripts submitted to this section are given priority in handling in the editorial office and in production. A Rapid Communication may be no longer than 3½ printed pages and must be accompanied by an abstract. Page proofs are sent to authors, but, because of the rapid publication schedule, publication is not delayed for receipt of corrections unless requested by the author.

Quantum-beat free-induction decay in Tm^{2+}:SrF_2: Fourier-transform ESR spectroscopy by optical means

T. Kohmoto, Y. Fukuda, M. Tanigawa, T. Mishina, and T. Hashi
Department of Physics, Faculty of Science, Kyoto University, Kyoto 606, Japan
(Received 6 June 1983)

We demonstrate, for the first time, a nanosecond Fourier-transform ESR experiment in solids achieved by optical means. ESR free-induction-decay signals in 0–100 Oe have been observed in the ground state of Tm^{2+}:SrF_2 as a new type of quantum beat generated by an optical excitation to the absorption band with a circularly polarized light pulse. The Fourier transform of the observed signals gives the ESR spectrum, and the origin of the decay is attributed to the superhyperfine interaction between the Tm^{2+} ion and neighboring fluorine nuclei.

Optically induced sublevel coherence plays an important role in laser spectroscopy. Recently several works have been done on the coherent transient phenomena of sublevel coherence and on the high-resolution sublevel spectroscopy.[1-6] These works suggest that the new type of magnetic resonance experiments can be carried out by using optically induced Zeeman coherence.

This paper reports on the first nanosecond Fourier-transform ESR experiment in solids achieved by optical means without any use of a microwave or rf source. ESR free-induction-decay (FID) signals were observed as ground-state quantum beats in a single crystal of Tm^{2+}:SrF_2 in low magnetic fields (0–100 Oe); the magnetization perpendicular to the static magnetic field (Zeeman coherence) is induced in the ground state by an optical excitation with a circularly polarized light pulse, and free precession of the magnetization is detected through optical anisotropy by using a polarization sensitive technique. These signals may be called "quantum-beat FID."[6]

In comparison with the usual quantum-beat experiments, our experiments differ in that the upper level of the relevant optical transition forms a $4f$-$5d$ band.[7] Magnetic circular dichroism and Faraday rotation of this transition[8] are responsible for the creation and detection of the signals. What we observed is the ground-state quantum beat generated by the optical excitation to the absorption band, which, to the authors' knowledge, have not been reported so far.

Complicated ESR FID signals with nanosecond decay times (10–30 nsec) were observed. The time resolution was far superior to that of the standard ESR apparatus. Using the data previously obtained[9-11] we identified the ESR spectrum and examined the origin of the decay or linewidth.

The ground state of the Tm^{2+} ion in the static magnetic field $\vec{H}$ is described by the spin Hamiltonian (neglecting the nuclear Zeeman interaction[9])

$$H = g\mu_B \vec{S}\cdot\vec{H} + A\vec{S}\cdot\vec{I} \ , \tag{1}$$

with effective electron spin $S=\frac{1}{2}$, nuclear spin $I(\mathrm{Tm})=\frac{1}{2}$, $g=3.445$, and $A=1102.5$ MHz, and the energy-level diagram is shown in the inset of Fig. 3. We suppose that the circularly polarized light pulse propagating along the z axis ($\perp\vec{H}$) excites the ion to the band, and the impact excitation condition is satisfied, i.e., the pulse width is much smaller than $1/\nu_{ij}$ $(i,j=1,2,3,4)$ and the relaxation times, where ν_{ij} is the frequency separation between levels i and j. The magnetization proportional to $\langle S_z\rangle$ is instantaneously created along the z axis because of the preferential depopulation of the ground substates, and begins to precess around the magnetic field. The generation of sublevel coherence by this process is analyzed in a similar way as in Ref. 12. We obtain the time evolution of $\langle S_z(t)\rangle$ governed by the Hamiltonian (1) under the initial condition that the population difference is created between the states with $S_z=\frac{1}{2}$ and $-\frac{1}{2}$, as

$$\langle S_z(t)\rangle \propto (\sin\alpha-\cos\alpha)^2(\cos 2\pi\nu_{12}t+\cos 2\pi\nu_{34}t) + (\sin\alpha+\cos\alpha)^2(\cos 2\pi\nu_{23}t+\cos 2\pi\nu_{14}t) \ , \tag{2}$$

where

$$\sin\alpha = a/\{2(a^2+4b^2)^{1/2}[(a^2+4b^2)^{1/2}+2b]\}^{1/2} \ ,$$

$a=\frac{1}{2}g\mu_B H$, $b=\frac{1}{4}A$, and the relaxations are not considered. The effect of optical coherence is ignored because of very fast optical dephasing. Equation (2) shows that sublevel coherences are created between level pairs 1-2, 2-3, 3-4, and 1-4 for which magnetic dipole transitions are allowed. The sublevel coherence is detected through the change of the polarization of linearly polarized probe light.

The wavelength of the probe light may be different from that of the pump light since the upper state is a band. This makes it easy to separate the signal from the strong pump pulse. The ions excited to the band immediately relax to the metastable state whose lifetime is several milliseconds.[13] Therefore the ions falling back to the ground state can be neglected in the nanosecond region where the FID signals are observed.

The experimental setup is shown in Fig. 1. The pump and probe pulses are provided by two independent nitrogen-laser-pumped dye lasers, which are triggered by hydrogen thyratrons (ITT F145 and 8613). The pump (circularly polarized) and probe (linearly polarized) beams are nearly collinear (parallel to the [111] axis) and focused on the sample (0.02%; 2 mm in thickness) in a liquid-helium cryostat. The waist sizes of the beams at the focus are ~ 100 μm. The wavelength, spectral width, pulse width, and peak power (in front of the Dewar) of the pump and probe pulses are 5865 Å, ~ 30 Å, 1 nsec, and 7 kW and 5400 Å, < 10 Å, 1 nsec, and 0.8 kW, respectively. The Glan-Thompson prisms are exactly crossed (extinction ratio with a sample between them is about 10^5), so that optically induced magnetization is detected as the change of the transmitted light intensity proportional to $\langle S_z \rangle^2$.

Figures 2(a)–2(d) show ESR FID (quantum-beat FID) signals for $H = 0$, 50, 75, and 100 Oe, obtained by plotting the transmitted light intensity versus probe delay times (from -5 to 45 nsec). An Ortec 467 time-to-pulse-height converter was used to eliminate the effect of the time jitter (~ 4 nsec) of the lasers. The FID signals were stored and averaged over ~ 5000 shots by a data acquisition system using a MZ-80 microcomputer. The signals were insensitive to the sense of the circular polarization of the pump pulse, and no temperature dependence was observed from 5 to 20 K.

Beat patterns of the signals in Figs. 2(b)–2(d) are due to simultaneous excitation of sublevel coherences at the frequencies ν_{12}, ν_{23}, ν_{34}, and ν_{14}. However, the oscillations at ν_{34} and ν_{14} (~ 1 GHz) cannot be detected in our experimental condition that the pulse widths are 1 nsec. Since we detect probe light intensity proportional to $\langle S_z \rangle^2$, these fast oscillating components give dc signals. The coherences at ν_{12} and ν_{23} give oscillating components of the signals at the frequencies $2\nu_{23}$, $2\nu_{12}$, $\nu_{23}+\nu_{12}$, and $\nu_{23}-\nu_{12}$.

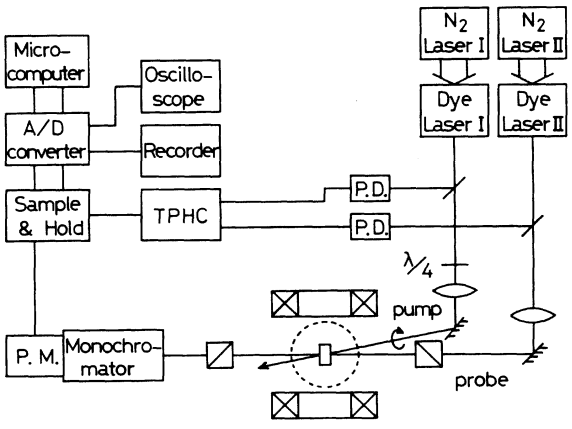

FIG. 1. Block diagram of the experimental setup.

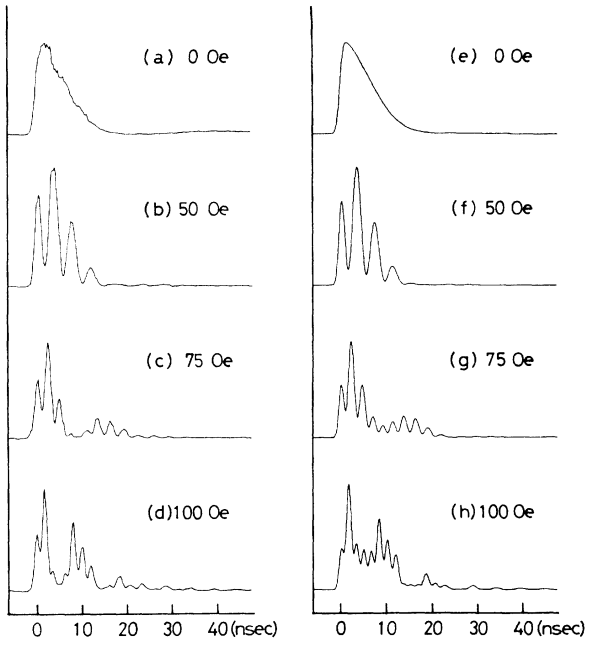

FIG. 2. Observed [(a)–(d)] and calculated [(e)–(h)] ESR FID (quantum-beat FID) signals for $H = 0$, 50, 75, and 100 Oe.

The Fourier spectrum of the observed signals shows these components. An example is shown in Fig. 3 ($H = 75$ Oe). The four peaks appear at the expected positions ($\nu_{23} = 210$ MHz and $\nu_{12} = 152$ MHz). The relative amplitude of the peaks at $2\nu_{12}$, $\nu_{23}+\nu_{12}$, and $2\nu_{23}$ is consistent with the theoretical prediction. The width of the peak at $2\nu_{23}$ is nearly twice as large as that at $2\nu_{12}$. Generally, the different coherences may have different decay times. Much simpler signals proportional to $\langle S_z \rangle$ are expected to be observed, if the Glan-Thompson prisms are deviated from an exactly crossed position. However, no reliable signal was obtained mainly because of a poor signal-to-noise ratio.

In order to analyze the beat pattern precisely and to obtain the decay time for each coherence, we performed computer calculations. It was reported that the cw ESR line shapes observed for Tm^{2+}:CaF_2 in 30–350 Oe were almost Gaussian and the width (~ 12 Oe) was independent of the magnetic field.[10] This observation suggests a model that the ESR line is inhomogeneously broadened by the static local

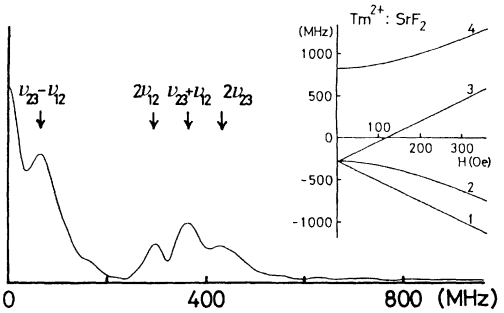

FIG. 3. Fourier spectrum of the ESR FID signal [Fig. 2(c)] at 75 Oe. The inset shows the energy-level diagram of the ground state of Tm^{2+} in SrF_2.

TABLE I. Experimental and theoretical values of T_2^* with corresponding linewidths.

H(Oe)		Experiment T_2^* (nsec)	Experiment FWHM[a] (MHz)	Theory T_2^* (nsec)	Theory FWHM (MHz)
50	(ν_{23}, ν_{14})	14	37	16	33
	(ν_{12}, ν_{34})	22	24	25	21
75	(ν_{23}, ν_{14})	14	38	15	35
	(ν_{12}, ν_{34})	26	20	29	19
100	(ν_{23}, ν_{14})	13	40	14	38
	(ν_{12}, ν_{34})	31	17	33	16
0		13	41	(14	38)

[a] Full width at half maximum.

field. According to this model we assigned the decay factor of the form $\exp[-(t/T_2^*)^2]$ to each oscillating term in Eq. (2) and assumed that the decay time T_2^* was inversely proportional to the effective g factor. The effective g factors ($\propto d\nu_{ij}/dH$) are equal for the transitions 1-2 and 3-4 (and for 2-3 and 1-4). The two effective g factors for 1-2 and 2-3 are not independent but related by the ratio $[(a^2+4b^2)^{1/2}+a]/[(a^2+4b^2)^{1/2}-a]$. The effect of the finite duration (~ 1 nsec) of the pump and probe pulses was taken into account by integrating Eq. (2) over the pulse width. The best fit between calculated values of $\langle S_z(t)\rangle^2$ and observed signals was obtained when the values of T_2^* listed in Table I were used. The corresponding linewidths in frequency are also tabulated. The linewidths in Oe are ~ 11 Oe which are nearly equal to those for Tm^2:CaF_2. Figures 2(e)–2(h) show the best-fit curves. The agreement is excellent for $H=0$, 50, and 75 Oe. The slight disagreement for $H=100$ Oe is probably due to the fact that the laser pulse has a temporal structure during 1 nsec, and that the signal is more sensitive to the structure when the precession period becomes short.

As the physical origin of T_2^* we consider the superhyperfine (shf) interaction (contact and dipole-dipole interactions) between the Tm^{2+} ion and surrounding fluorine nuclei. The Hamiltonian and the values of coupling constants are known up to the fourth nearest fluorine shell in SrF_2.[11] The nuclear Zeeman term can be neglected in our case ($H \lesssim 100$ Oe). The Tm^{2+}-Tm^{2+} interaction is also neglected because of the small concentration of the sample. We calculated second moments of the ESR transitions for $H=50$, 75, and 100 Oe where the contribution of shf interaction is sufficiently small compared with ν_{12}, ν_{23}, ν_{34}, and ν_{14}.[14] Assuming a Gaussian line shape we obtain theoretical values of the decay times and linewidths as in Table I. The theoretical values are independent of the direction of the magnetic field relative to the crystalline axes. The agreement between the theoretical and experimental values is satisfactory, which indicates that the origin of the decay of the FID signals (at $H=50$, 75, and 100 Oe) is the shf interaction between the Tm^{2+} ion and the surrounding fluorine nuclei.

In the zero magnetic field, levels 1, 2, and 3 are degenerate ($\nu_{12}=\nu_{23}=0$, $\nu_{14}=\nu_{34}=\nu_0=1.1$ GHz). The optical excitation induces zero-frequency coherences between levels 1-2 and 2-3 and fast oscillating ones between 1-4 and 3-4. Both of these coherences give dc signals. The second-moment approach is not appropriate in this case. Then we calculated the trace of the square of the shf Hamiltonian, which gives a measure of the broadening (energy distribution) of the degenerate level ($F=1$). Level 4 ($F=0$) is not broadened because $\langle\vec{S}\rangle=0$. The decay time estimated from the broadening of the level $F=1$ is listed in Table I, where Gaussian distribution is assumed. The agreement with the experimental value is satisfactory for the crudeness of the model.

When a small magnetic field was applied along the light beam, we observed much stronger signals due to the optically induced longitudinal magnetization whose lifetime T_1 was $\sim 10^{-1}$ sec. These signals exhibited anomalous behaviors when the magnetic field was comparable to the local field (10–20 Oe).

The experiment described here demonstrates the versatility of quantum-beat FID for high-sensitive Fourier-transform ESR spectroscopy in the nanosecond region. The time resolution is determined by the laser pulse widths independent of the response times of the detectors or electronics. The time resolution may be easily extended to the picosecond region by using picosecond light pulses. The steady-state population difference of sublevels is not necessary in this method in contrast to the usual ESR experiment. ESR frequencies in a wide range (0 ~ few GHz) can be covered simply by changing magnetic field. The present method should be applicable to various impurity-ion solids and other materials. Optically induced ESR FID was previously detected magnetically in a sample with a sharp optical line.[15] We have shown that the sharp optical line is not necessary, which greatly extends the variety of samples to be studied. The observation of optically induced ESR echoes (quantum-beat echoes[4]) is attractive because it can extract homogeneous broadening and detect shf spectrum via echo envelope modulation.

ACKNOWLEDGMENTS

We would like to thank Dr. C. H. Anderson of RCA Laboratories for kindly providing us with the sample crystals. This work was supported in part by the Shimazu Science Foundation.

[1]T. Endo, S. Nakanishi, T. Muramoto, and T. Hashi, Opt. Commun. 43, 359 (1982).

[2]H. Harde, H. Burggraf, J. Mlynek, and W. Lange, Opt. Lett. 6, 290 (1981).

[3]Y. Fukuda, J. Hayashi, K. Kondo, and T. Hashi, Opt. Commun. 38, 357 (1981).

[4]Y. Fukuda, K. Yamada, and T. Hashi, Opt. Commun. 44, 297 (1983).

[5]J. Mlynek, N. C. Wong, R. G. DeVoe, E. S. Kintzer, and R. G. Brewer, Phys. Rev. Lett. 50, 993 (1983).

[6]R. M. Shelby, A. C. Tropper, R. T. Harley, and R. M. Macfarlane, Opt. Lett. 8, 304 (1983).

[7]Z. J. Kiss, Phys. Rev. 127, 718 (1962).

[8]C. H. Anderson, H. A. Weakliem, and E. S. Sabisky, Phys. Rev. 143, 223 (1966).

[9]C. H. Anderson and E. S. Sabisky, in *Physical Acoustics,* edited by W. P. Mason and R. N. Thurston (Academic, New York, 1971), Vol. VIII, Chap. 1, and references therein.

[10]E. B. Aleksandrov and V. S. Zapasskii, Fiz. Tverd. Tela (Leningrad) 19, 3083 (1977) [Sov. Phys. Solid State 19, 1802 (1977)].

[11]W. Hayes and P. H. S. Smith, J. Phys. C 4, 840 (1971).

[12]K. Yamada, Y. Fukuda, and T. Hashi, J. Phys. Soc. Jpn. 50, 592 (1981).

[13]E. S. Sabisky and C. H. Anderson, Phys. Rev. 148, 194 (1966).

[14]R. F. Wenzel, Phys. Rev. B 1, 3109 (1970).

[15]Y. Takagi, Y. Fukuda, K. Yamada, and T. Hashi, J. Phys. Soc. Jpn. 50, 2672 (1981).